PCCP

RSC Publishing

PAPER

View Article Online
View Journal | View Issue

Porphyrin sensitizers with π-extended pull units for dye-sensitized solar cells†

Cite this: *Phys. Chem. Chem. Phys.*, 2013, **15**, 8409

Nagannagari Masi Reddy,[a] Tsung-Yu Pan,[b] Yesudoss Christu Rajan,[a] Bo-Cheng Guo,[a] Chi-Ming Lan,[b] Eric Wei-Guang Diau*[b] and Chen-Yu Yeh*[a]

Received 28th March 2013,
Accepted 28th March 2013

DOI: 10.1039/c3cp51327k

www.rsc.org/pccp

New π-extended porphyrin dyes **YD26–YD29** with long alkoxyl chains at the *ortho* positions of the *meso*-phenyls, and *meta* di-*tert*-butylphenyl-substituted porphyrins **YD12–CN**, and **YD13–CN** were synthesized for dye-sensitized solar cells, and their optical, electrochemical and photovoltaic properties were investigated and compared with those of **YD12** and **YD13**. The absorption spectra of **YD26–YD29** showed a slight red shift of Soret bands and blue shift of Q bands as compared to the *meta*-substituted porphyrins due to the electron-donating effects of dioctyloxy substituents at the *ortho*-positions of the *meso*-phenyl rings. Replacement of the carboxyl with a cyanoacrylic acid as the anchoring group results in significant broadening and red shifts of the absorptions, which is due to the strong electronic coupling between the pull unit and the porphyrin ring facilitated by the C≡C triple bond. The electrochemical studies and quantum-chemical calculations (DFT) indicated that the *ortho* alkoxy-substituted sensitizers exhibit lower oxidation potential, *i.e.* a higher HOMO energy level, and their HOMO–LUMO gaps are comparable to the *meta*-substituted analogues. The photovoltaic measurements confirmed that the *ortho*-octyloxy groups in the two *meso*-phenyls of **YD26** and **YD27** play a significant role in preventing dye aggregation thereby enhancing the corresponding short-circuit current density and open-circuit voltage. The power conversion efficiency (η) of **YD26** is 8.04%, which is 11% higher than that of **YD12**, whereas the efficiency of **YD27** is 6.03%, which is 135% higher than that of **YD13**. On the other hand, the poor performance of **YD28** and **YD29** is due to the floppy structural nature and limited molecular rigidity of the cyanoacrylic acid anchor.

Introduction

Depletion of fossil fuels and the increasing demand for energy creates an urgent need to discover alternatives for the world's conventional energy supplies.[1] Hence, further research to explore alternative, safe and renewable sources of energy is extremely important.[2] Among all renewable energy technologies, photovoltaics which utilize solar energy is believed to be the most promising one. Solar energy, one of the most abundant and renewable sources of energies, is poised to play a great role, as the amount of energy emitted from sun to earth is several thousand times higher than the global requirement.[3] The photovoltaic devices made by silicon semiconductors are nowadays used for the direct conversion of sunlight into electrical energy. However, this type of solar cells has major limitations due to difficulties related to large scale production and high fabrication cost.

Inspired by the pioneering work done by Grätzel and co-workers over the past decades, dye-sensitized solar cells[4] (DSCs) have attracted much attention with the advantages of high energy conversion efficiency, low cost together with facile fabrication and are nowadays used as promising alternatives to the conventional silicon-based solar cells.[5] Ruthenium polypyridyl complex photosensitizers such as **N719**, **N3** and the black dyes show a solar-to-energy conversion efficiency of up to 11% under standard illumination (AM 1.5).[6] However, the limited availability, complicated purification and environmental concerns of the ruthenium-based dyes prompted researchers to search for cheaper and safer organic dyes. Organic sensitizers have many advantages such as large molar extinction coefficient, control of absorption wavelength, simple design and synthesis, lower cost and great flexibility in structural tuning with high stability than other photosensitizers.

Hence, recently many studies have been performed aimed at the development of highly efficient and stable organic

[a] *Department of Chemistry and Center of Nanoscience and Nanotechnology, National Chung Hsing University, Taichung, 402, Taiwan. E-mail: cyyeh@dragon.nchu.edu.tw; Fax: +886-4-2286-2547*

[b] *Department of Applied Chemistry and Institute of Molecular Science, National Chiao Tung University, Hsinchu, 300, Taiwan. E-mail: diau@mail.nctu.edu.tw; Fax: +886-3-572-3764*

† Electronic supplementary information (ESI) available: Experimental details. See DOI: 10.1039/c3cp51327k

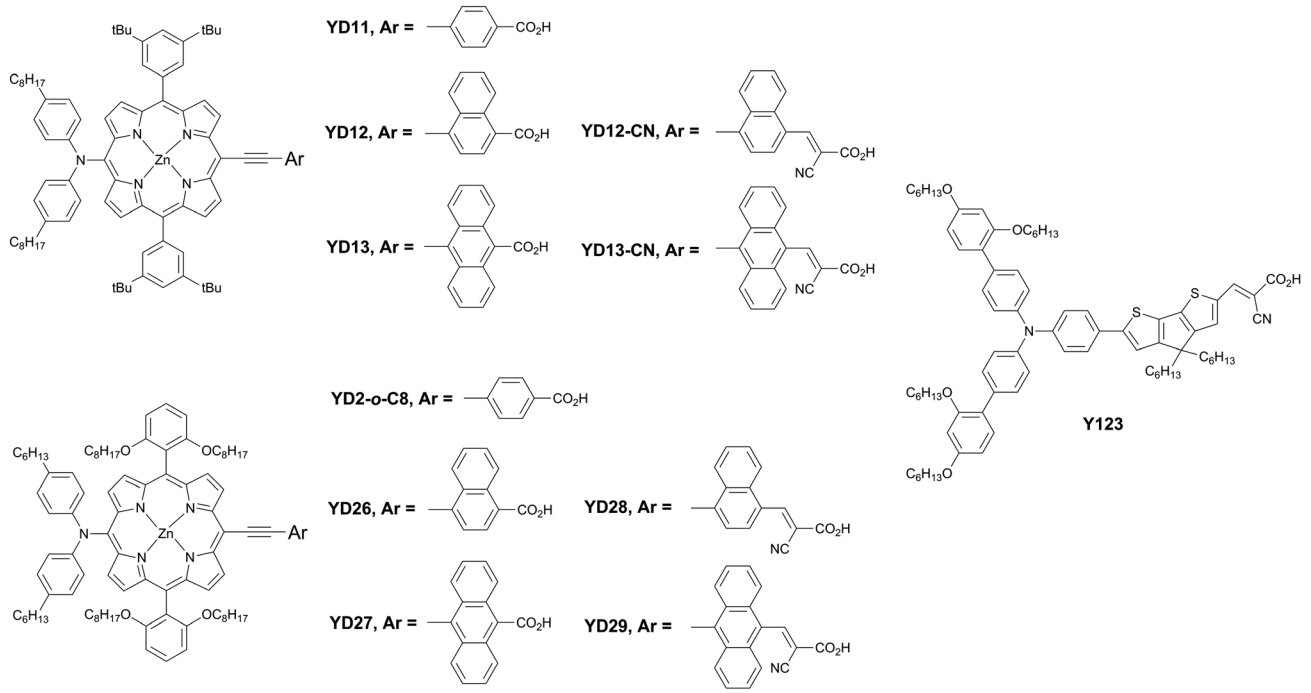

Fig. 1 Molecular structures of **YD** series porphyrins and **Y123**.

sensitizers. As a result, a number of organic dyes without metals[7] or with inexpensive metal and π-conjugated[8] molecules, hemicyanine,[9] coumarin,[10] indoline,[11] thiophene,[12] perylene,[13] cyanine[14] and triarylamine[15] DSCs have been intensively studied. The most efficient organic dyes have reached encouraging solar power conversion efficiencies up to 10%.

Among numerous non-ruthenium dyes, porphyrins and the related derivatives are widely studied potential sensitizers for DSCs, due to their structural similarity to chlorophylls in natural photosynthetic systems as well as their intense Soret bands in the range 400 to 450 nm and moderate Q bands between 500 and 650 nm.[16] More importantly, their optical, photophysical and electrochemical properties can be easily modulated by peripheral substitutions and/or metal complexation. However, most of these porphyrin-based dyes display lower efficiency due to the formation of severe dye aggregates and insufficient light-harvesting ability in the region between the Soret and Q bands. One of the approaches to improving the cell performance of the porphyrin dyes is to extend their π-system, which leads to broadening and red shifts of the absorptions, thus enhancing their light-harvesting efficiency. Officer *et al.* synthesized β-carboxyl-substituted monomer and multiporphyrin arrays used for testing photovoltaic solar cells.[17] Imahori and coworkers reported the synthesis and photovoltaic properties of various unsymmetrical, π-elongated naphthyl fused porphyrins which modulate the electronic structures of the porphyrin dye to match the light harvesting properties of the solar spectrum thereby consequently doubling the cell performance of the naphthyl-fused porphyrin than the unfused counterpart.[18] The best performance of the dyes depends upon the broadening of light absorption capability, fast electron injection from the excited dye to the conduction band and finally retardation in charge recombination.[19,20]

In general, simple porphyrin macrocycles with a large planar-system suffer from severe dye aggregation. Our previous reports on porphyrin sensitizers showed that attachment of *tert*-butyl groups to the *meta*-positions of the peripheral phenyls in the *meso*-positions of the porphyrin can moderately reduce dye aggregation.[21] In the push–pull porphyrins,[21–26] one *meso*-position of the porphyrin core is attached by a strong electron donor such as triphenylamine or diphenylamine opposite to the *meso*-substituted linker *via* an ethynyl bridge with a carboxylic acid serving as an anchoring group for dye adsorption to the surface of TiO_2. Such a push–pull structural feature is believed to be responsible for the excellent cell performance of the devices. To improve the device performance, the phenyl bridge between the carboxyl and porphyrin ring in **YD11** was modified with a naphthalene unit (**YD12**) to increase π-extension, resulting in a red-shift and broadening of the absorptions.[21] However, the replacement of the phenyl group with an even more π-extended anthracene bridge (**YD13**) decreased power conversion efficiency due to molecular aggregation.[23] More recently, **YD2–*o*–C8** with octoxyl groups at the *ortho*-positions of the peripheral phenyls, attached to the *meso*-positions of the porphyrin core has achieved a record efficiency of 12.3% when co-sensitized with an organic dye **Y123**.[26] Based on our previous work we thus aim to synthesize naphthalene- and anthracene-bridged porphyrins with a carboxyl or cyanoacrylic acid as the anchoring group and to investigate the structure–photovoltaic property relationship of these porphyrin dyes. The molecular structures of these porphyrins **YD12**, **YD13**, **YD12–CN**, **YD13–CN**, **YD26–YD29** studied in this work are shown in Fig. 1.

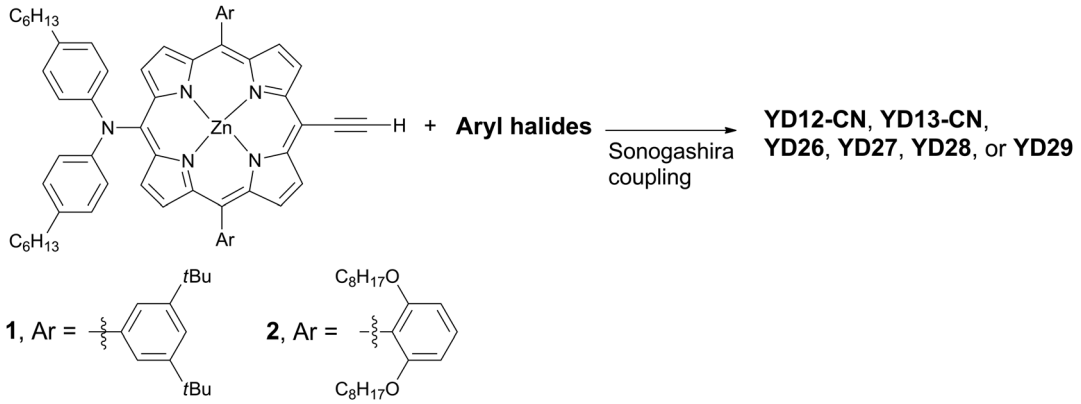

Scheme 1 Synthesis of novel porphyrin dyes. Reagent and conditions: $Pd_2(dba)_3$, $AsPh_3$, THF/NEt_3, refluxed for several hours.

Results and discussion

As mentioned, replacement of *meta*-substituted *tert*-butyl groups by octoxyl groups at the *ortho*-positions of the peripheral phenyl rings in the *meso*-positions of porphyrin core can effectively reduce dye aggregation in porphyrin **YD2–*o*–C8**. In addition, the alkyl chains form a hydrophobic environment to successfully block the approach of the electrolyte to the surface of TiO_2 and reduce charge recombination, thus significantly enhancing the power conversion efficiency.[26] The naphthalene- and anthracene-bridged porphyrins **YD26** and **YD27** were designed based on the same concept. It is also desirable to study the cyanoacrylic acid analogues **YD12–CN**, **YD13–CN**, **YD28**, and **YD29** since it has been widely used as the anchoring group in the most efficient organic dyes. The syntheses of these porphyrins are straightforward by employing Sonogashira coupling of precursor **1** or **2** with the appropriate halides of the pull unit as outlined in Scheme 1. The detailed experimental procedures for the porphyrin dyes and intermediates are given in ESI.†

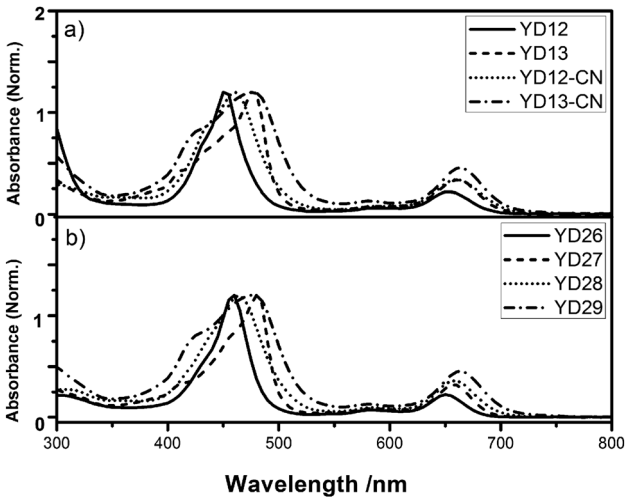

Fig. 2 Absorption spectra of porphyrin dyes (a) **YD12**, **YD13**, **YD12–CN**, and **YD13–CN**; (b) **YD26**, **YD27**, **YD28** and **YD29** in THF.

Absorption and emission spectra

The absorption spectra of these porphyrins in THF solvent are given in Fig. 2 and the corresponding spectral data are summarized in Table 1. Absorption spectra of all these porphyrin dyes exhibit maxima attributed to π–π^* transitions in the range 400–550 nm for the Soret band and 550–750 nm for the Q bands. Replacement of *meta*-substituted *tert*-butyl groups by octoxyl groups at the *ortho*-positions of the peripheral phenyls cause slight changes on the absorption features of the porphyrin dyes. The Soret bands of **YD26–YD29** are slightly red-shifted whereas their Q bands are slightly blue-shifted as compared with the di-*tert*-butylphenyl-substituted counterparts. This is ascribed to the electronic effects of the two electron-donating dioctyloxy substituents at the *ortho*-positions of the *meso*-phenyl ring. A similar trend was also observed in fluorescence, the emission maxima for porphyrin dyes **YD26–YD29** are blue-shifted. The absorption properties of these porphyrin dyes are expected to be significantly changed as the structures of the pull units are varied because there is strong electronic coupling between the pull unit and the porphyrin ring, efficiently mediated by the C≡C triple bond. The anthracene-bridged porphyrins **YD13** and **YD27** show red shifts and broadening on both Soret and Q bands compared to the corresponding naphthalene-bridged analogues **YD12** and **YD28** due to π-extension. The use of cyanoacrylic acid instead of carboxylic acid results in slight red shifts and significant broadening on the absorptions in both naphthalene- and anthracene-bridged systems. Similar to the absorption spectra, the emission spectra also red-shifted as the π-bridge is extended and/or the strong pull unit cyanoacrylic acid is incorporated to the porphyrin macrocycles as compared to those of their corresponding carboxyl counterparts. The detailed fluorescence data are listed in the Table 1.

Electrochemical properties and energy levels

The redox potentials of these porphyrin dyes were determined by using cyclic voltammetry under ambient conditions as summarized in Table 1. All porphyrins exhibited reversible waves for the first oxidation potential, corresponding to the HOMO energy of the dye, at a potential greater than that of the I^-/I_3^- (0.35 V) couple. The first oxidation waves were observed

Table 1 Spectral and electrochemical data for dyes[a]

Porphyrin	Absorption, λ_{max}/nm	Emission, λ_{max}/nm[b]	Oxidation, $E_{1/2}$/V[c]	Reduction, $E_{1/2}$/V[c]
YD12	452, 580, 652	680	+0.92 (0.12), +1.30[d]	−1.10 (0.12)
YD13	479, 582, 661	687	+0.90 (0.11), +1.37[d]	−1.17 (0.12)
YD12–CN	460, 585, 657	687	+0.93 (0.13), +1.24[d]	−1.07 (0.14)
YD13–CN	481, 582, 661	695	+0.91 (0.08), +1.30[d]	−1.15 (0.13)
YD26	456, 583, 648	668	+0.83 (0.12), +1.35[d]	−1.25 (0.12)
YD27	481, 584, 657	676	+0.80 (0.12), +1.29[d]	−1.28 (0.14)
YD28	464, 584, 655	679	+0.82 (0.12), +1.35[d]	−1.25[e]
YD29	481, 582, 660	689	+0.80 (0.12), +1.29[d]	−1.23[e]

[a] Absorption and emission data were measured in THF at 25 °C. Electrochemical measurements were performed at 25 °C in THF containing $TBAPF_6$ (0.1 M) as supporting electrolyte, except for **YD13–CN**, of which the electrochemical measurements were performed in CH_2Cl_2. Potentials measured *vs.* ferrocene/ferrocenium (Fc/Fc^+) couple were converted to normal hydrogen electrode (NHE) by addition of +0.63 V. [b] The excitation wavelengths were 652, 655, 661, 662, 648, 653, 655 and 661 nm for **YD12**, **YD12–CN**, **YD13**, **YD13–CN**, **YD26**, **YD27**, **YD28** and **YD29y**, respectively in THF. [c] The numbers in parentheses represent peak-to-peak separations of the redox waves. [d] Irreversible process E_{pa}. [e] Irreversible process E_{pc}.

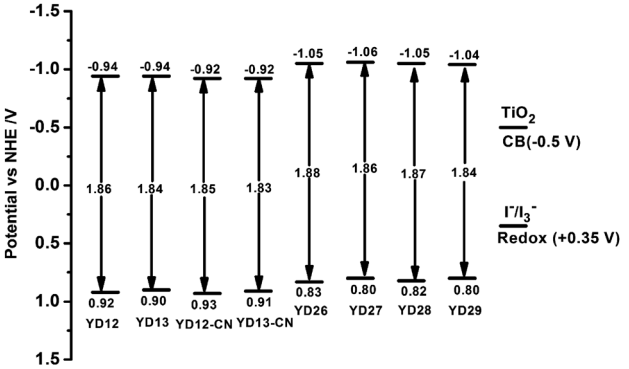

Fig. 3 Energy level diagrams of porphyrins **YD12–YD29**.

in the range +0.80 to +0.83 V *versus* normal hydrogen electrode (NHE) for **YD26–YD29**. These values are lower than those of di-*tert*-butylphenyl-substituted analogues because of the electron-donating alkoxyl substituents on the *meso*-phenyl rings (Table 1). Similarly, cathodic shifts of the reduction potentials for **YD26–YD29** relative to those of *meta*-substituted phenyl counterparts reflect a lifting of the lowest unoccupied molecular orbital (LUMO) level and are a manifestation of the same effects. Variation of the pull units for the porphyrins with the same peripheral phenyls only slightly influences the first oxidation potential. This is because the electron density for the HOMO is located on the push unit and porphyrin ring. However, more pronounced changes on the first reduction potential were observed since the electron distribution of the LUMO is mainly located on the pull unit. These electrochemical results are consistent with those obtained from the density-functional theory (DFT) calculations discussed in the next section.

The potentials measured in THF *vs.* Fc^+/Fc were converted to normal hydrogen electrode (NHE) by addition of +0.63 V. The energy levels for the HOMO and excited singlet states of the porphyrins used in this study were derived from the equation $E_{0-0^*} = E_{ox1} - E_{0-0}$, in which E_{ox1} is the first oxidation potential of a porphyrin dye and E_{0-0} represents the energy gap between highest occupied molecular orbital to lowest unoccupied molecular orbital which is estimated from the intercept of the normalized absorption and emission spectra in THF. The energy levels of these porphyrins are depicted in Fig. 3. The HOMO level of these dyes are more positive than the I^-/I_3^- redox electrolyte (+0.35 V *vs.* NHE), indicating that there is enough driving force for the dye regeneration. On the other hand, the calculated $E_{0\text{-}0^*}$ values are all more negative than the conduction edge (CB) (−0.50 V *vs.* NHE) of TiO_2. Therefore, these types of sensitizers have sufficient driving force for electron injection to TiO_2.

Quantum-chemical calculations

To gain insight into the electron distribution of the frontier and other close-lying orbitals, we performed quantum-chemical calculations on these porphyrins using the DFT approach at the RB3LYP/6-31G* level (Spartan 08 package). To simplify the computations, the alkyl groups of phenyl rings were replaced by hydrogen atoms and methyl groups for the *meta*- and *ortho*-substituted phenyls. Fig. S1 and S2 (ESI†) show an energy-level diagram and the corresponding molecular orbitals for these porphyrin dyes. Replacement of *meta*-substituted di-*tert*-butyl groups with *ortho*-substituted octoxyl groups on peripheral phenyls of the porphyrin core, resulted in an increase of both HOMO and LUMO energy levels and the HOMO–LUMO gaps being almost unchanged, which are in accordance with the potential feature shown in Fig. 3. The electronic densities of these porphyrins are mainly located on the π-system of the porphyrin and the diarylamine at the HOMO and HOMO − 1. The electronic distributions of the frontier orbitals for compounds **YD12** and **YD13** resemble those of **YD26** and **YD27** because of the structural similarity. Similarly, **YD12–CN** and **YD13–CN** show electron distributions in accordance with those of **YD28** and **YD29**, respectively. The electron distributions of the LUMO for porphyrins **YD12** and **YD13** are mainly located at the naphthalene and anthracene linkers, respectively. The same trend was observed for **YD26** and **YD27** due to similarity in the structures. When a strong pull unit cyanoacrylic acid is introduced to the naphthalene and anthracene the electron densities of the LUMO for **YD12–CN**, **YD13–CN**, **YD28** and **YD29** are mainly located on both the π-linker and anchoring group.

Photovoltaic characteristics

The photovoltaic properties of four naphthalene-bridged porphyrins **YD12**, **YD12–CN**, **YD26** and **YD28**, and four anthracene-bridged porphyrins **YD13**, **YD13–CN**, **YD27** and **YD29** were investigated using the TiO_2 electrodes fabricated at the same film thickness (10 + 4 μm) under identical experimental conditions.[21] Corresponding current–voltage characteristics and action spectra of incident photo-to-current conversion efficiency (IPCE) are displayed in Fig. 4 and 5, respectively, with the results of naphthalene and anthracene-bridged porphyrins shown as plots (a) and (b) in each figure. The obtained photovoltaic parameters of the eight devices are summarized in Table 2. For the naphthalene-bridged porphyrins, the *ortho*-substituted long alkoxyl chains in the two *meso*-phenyls of **YD26** play a key role to prevent dye aggregation so

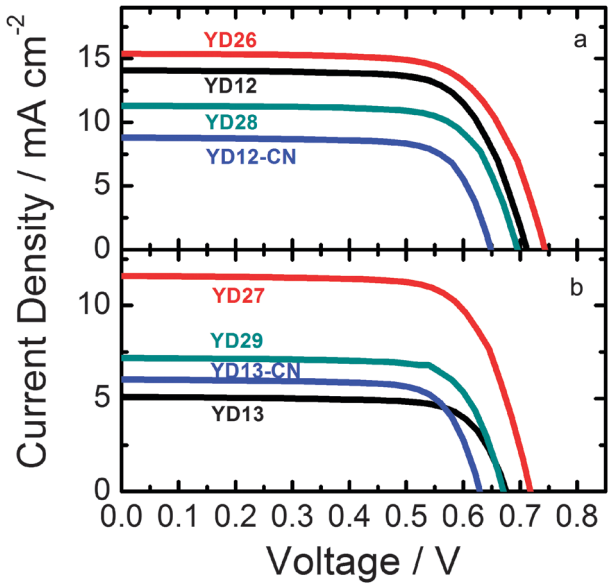

Fig. 4 Current–voltage characteristics of DSSCs based on various porphyrin dyes: (a) naphthalene-based series and (b) anthracene-based series.

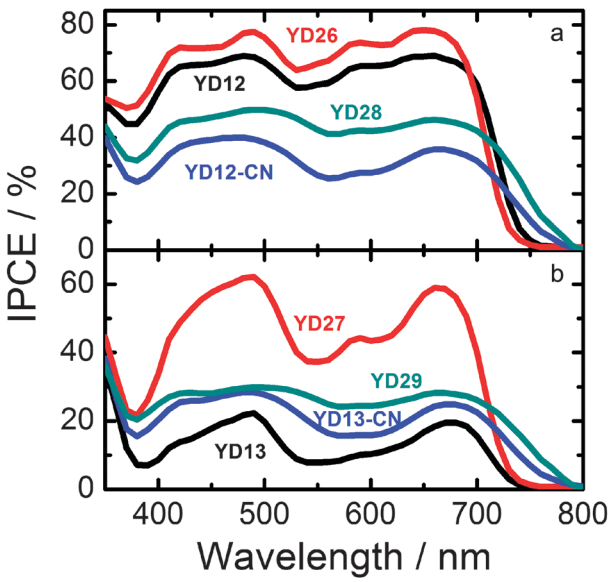

Fig. 5 Action spectra of incident photon-to-current conversion efficiency (IPCE) of DSSCs based on various porphyrin dyes: (a) naphthalene-based series and (b) anthracene-based series.

that both short-circuit current density (J_{SC}) and open-circuit voltage (V_{OC}) were significantly enhanced for **YD26** than for **YD12**. As a result, the power conversion efficiency (η) of **YD26** reached 8.04%, which is ~11% higher than that of **YD12** (7.23%). This phenomenon is consistent with the **YD2** system for which the **YD2–*o*–C8** device outperformed the **YD2** device with a similar molecular design.[2] For the **YD12–CN** device with the cyanoacrylic acid moiety as an anchoring group, both J_{SC} and V_{OC} were significantly reduced so that its performance became the poorest one among all the naphthalene-bridged porphyrin devices. Even though the long alkoxyl chains were involved in **YD28** in order to reduce the extent of dye aggregation, the improvement was very limited for this cyanoacrylic acid-based porphyrin. One possibility for the poor performance of **YD28** with respect to that of **YD26** is the floppy structural nature of the porphyrin, which might lead to **YD28** to tilt down the TiO_2 surface for an efficient charge recombination to occur.[19]

Table 2 Photovoltaic parameters under global AM 1.5 irradiation for DSSCs adsorbed on nanocrystalline TiO_2 anodes

Porphyrin	J_{SC}/mA cm^{-2}	V_{OC}/V	FF	η/%
YD12	14.06	0.713	0.721	7.23
YD13	5.09	0.679	0.743	2.57
YD12–CN	8.79	0.651	0.748	4.28
YD13–CN	6.03	0.632	0.752	2.86
YD26	15.37	0.745	0.702	8.04
YD27	11.59	0.720	0.723	6.03
YD28	11.30	0.696	0.737	5.80
YD29	7.17	0.673	0.755	3.64

The devices made of **YD13** were found to perform extremely poorly due to a serious problem of dye aggregation on the TiO_2 surface that significantly reduced the efficiency of electron injection from the excited state of the dye molecule to the conduction band of TiO_2.[23] However, the *ortho*-substituted long alkoxyl chains in **YD27** exhibited dramatic effects to decrease the degree of dye aggregation so that the IPCE values of **YD27** were significantly improved by a factor of three over those of **YD13**. As a result, J_{SC} of the **YD27** device was improved by more than a factor of two over that of the **YD13** device. Moreover, V_{OC} of **YD27** was greater than that of **YD13** by ~40 mV, and this improvement is understood as being due to both effects of up-shifted potential band edge and retarded charge recombination for the former compared to the latter.[27] Therefore, the device performance of **YD27** reached η = 6.03%, which is remarkably improved by 135% compared with that of **YD13**. On the other hand, the improvement of the performance with the design of *ortho*-substitution for the cyanoacrylic acid-based porphyrin **YD29** over that of **YD13–CN** was very limited as in the case of **YD28** *vs.* **YD12–CN**, confirming that molecular rigidity plays a key role to improve the device performance for porphyrin-sensitized solar cells.

Conclusions

We have synthesized new naphthalene- and anthracene-bridged porphyrins with carboxylic and cyanoacrylic acid anchoring group for DSCs applications. The absorption and emission bands of *ortho* dioctyloxy-substituted porphyrins **YD26** and **YD27** are slightly red shifted for the Soret band and slightly blue-shifted for the Q bands compared to the *meta*-substituted porphyrins. The anthracene-bridged porphyrins, in addition to red shifts, showed broadening on both Soret and Q bands than naphthalene analogues due to π-extension. Furthermore, the use of cyanoacrylic acid instead of carboxylic acid as the anchoring group causes significant broadening and red shifts of the absorptions. However, the photovoltaic performance of the cyanaoacrylic acid-based porphyrins is poorer compared to carboxyl-based analogues

due to the lack of molecular rigidity.[25] Electrochemical studies and DFT calculations revealed that the HOMO–LUMO band gaps are almost unchanged upon substitution of the *meta*-di-*tert*-butyl with *ortho*-dioctoxyl groups and the redox potentials of the alkoxy-substituted porphyrins are more positive than the corresponding *meta*-substituted analogues. Additionally, the octyloxy substituents form a hydrophobic environment to reduce charge recombination and suppress dye aggregation on the surface of TiO_2, thereby strikingly increasing the power conversion efficiencies for **YD26** (8.04%) and **YD27** (6.03%) compared to those of their meta-substituted counterparts **YD12** (7.23%) and **YD13** (2.57%).

Acknowledgements

We are grateful for support from the National Science Council of Taiwan and the Ministry of Education of Taiwan, under the ATU program.

Notes and references

1 (*a*) N. Robertson, *Angew. Chem., Int. Ed.*, 2008, **47**, 1012–1014; (*b*) R. Eisenberg and D. G. Nocera, *Inorg. Chem.*, 2005, **44**, 6799–6801; (*c*) N. Lewis and D. Nocera, *Proc. Natl. Acad. Sci. U. S. A.*, 2006, **103**, 15729–15735.

2 N. Oreskes, *Science*, 2004, **306**, 1686.

3 M. Grätzel, *Nature*, 2001, **414**, 338–344.

4 (*a*) B. O'Regan and M. Grätzel, *Nature*, 1991, **353**, 737–740; (*b*) M. K. Nazeeruddin, A. Kay, I. Rodicio, R. Humphry-Baker, E. Müller, P. Liska, N. Vlachopoulos and M. Grätzel, *J. Am. Chem. Soc.*, 1993, **115**, 6382–6390; (*c*) M. K. Nazeeruddin, P. Péchy, T. Renouard, S. M. Zakeeruddin, R. Humphry-Baker, P. Comte, P. Liska, L. Cevey, E. Costa, V. Shklover, L. Spiccia, G. B. Deacon, C. A. Bignozzi and M. Grätzel, *J. Am. Chem. Soc.*, 2001, **123**, 1613–1624.

5 (*a*) Y. Ooyama and Y. Harima, *Eur. J. Org. Chem.*, 2009, 2903–2934; (*b*) M. Grätzel, *Acc. Chem. Res.*, 2009, **42**, 1788–1798; (*c*) T. W. Hamann, R. A. Jensen, B. F. Martinson, H. V. Ryswyk and J. T. Hupp, *Energy Environ. Sci.*, 2008, **1**, 66–78; (*d*) N. Robertson, *Angew. Chem., Int. Ed.*, 2006, **45**, 2338–2345.

6 (*a*) L. Han, A. Islam, H. Chen, C. Malapaka, B. Chiranjeevi, S. Zhang, X. Yang and M. Yanagida, *Energy Environ. Sci.*, 2012, **5**, 6057–6060; (*b*) F. Gao, Y. Wang, D. Shi, J. Zhang, M. Wang, X. Jing, R. Humphry-Baker, P. Wang, S. M. Zakeeruddin and M. Grätzel, *J. Am. Chem. Soc.*, 2008, **130**, 10720–10728; (*c*) Y. Cao, Y. Bai, Q. Yu, Y. Cheng, S. Liu, D. Shi, F. Cao and P. Wang, *J. Phys. Chem. C*, 2009, **113**, 6290–6297.

7 A. Mishra, M. K. R. Fischer and P. Bäuerle, *Angew. Chem., Int. Ed.*, 2009, **48**, 2474–2499.

8 (*a*) Q. Wang, W. M. Campbell, E. E. Bonfantani, K. W. Jolley, D. L. Officer, P. J. Walsh, K. Gordon, R. H-Baker, M. K. Nazeeruddin and M. Grätzel, *J. Phys. Chem. B*, 2005, **109**, 15397–15409; (*b*) S. Hayashi, M. Tanaka, H. Hayashi, S. Eu, T. U. Meyama, Y. Matano, Y. Araki and H. Imahori, *J. Phys. Chem. C*, 2008, **112**, 15576–15585; (*c*) N. Koumura, Z. S. Wang, S. Mori, M. Miyashita, E. Suzuki and K. Hara, *J. Am. Chem. Soc.*, 2006, **128**, 14256–14257; (*d*) S. Eu, S. Hayashi, T. Umeyama, A. Oguro, M. Kawasaki, N. Kadota, Y. Matano and H. Imahori, *J. Phys. Chem. C*, 2007, **111**, 3528–3537; (*e*) A. Hagfeldt, G. Boschloo, L. Sun, L. Kloo and H. Pettersson, *Chem. Rev.*, 2010, **110**, 6595–6663; (*f*) J. N. Clifford, E. Martínez-Ferrero, A. Viterisi and E. Palomares, *Chem. Soc. Rev.*, 2011, **40**, 1635–1646.

9 (*a*) Q.-H. Yao, L. Shan, F.-Y. Li, D.-D. Yin and C.-H. Huang, *New J. Chem.*, 2003, **27**, 1277–1283; (*b*) Y.-S. Chen, C. Li, Z.-H. Zeng, W.-B. Wang, X.-S. Wang and B.-W. Zhang, *J. Mater. Chem.*, 2005, **15**, 1654–1661.

10 (*a*) K. Hara, K. Sayama, Y. Ohga, A. Shinpo, S. Suga and H. Arakawa, *Chem. Commun.*, 2001, 569–570; (*b*) K. Hara, M. Kurashige, Y. Danoh, C. Kasada, A. Shinpo, S. Suga, K. Sayama and H. Arakawa, *New J. Chem.*, 2003, **27**, 783–785; (*c*) Z.-S. Wang, Y. Cui, Y. Dan-oh, C. Kasada, A. Shinpo and K. Hara, *J. Phys. Chem. C*, 2007, **111**, 7224–7230.

11 (*a*) T. Horiuchi, H. Miura and S. Uchida, *Chem. Commun.*, 2003, 3036–3037; (*b*) T. Horiuchi, H. Miura, K. Sumioka and S. Uchida, *J. Am. Chem. Soc.*, 2004, **126**, 12218–12219; (*c*) S. Ito, S. M. Zakeeruddin, R. Humphry-Baker, P. Liska, R. Charvet, P. Comte, M. K. Nazeeruddin, P. Péchy, M. Takata, H. Miura, S. Uchida and M. Grätzel, *Adv. Mater.*, 2006, **18**, 1202–1205.

12 (*a*) S. Kim, H. Choi, D. Kim, K. Song, S. O. Kang and J. Ko, *Tetrahedron*, 2007, **63**, 9206–9212; (*b*) S. Kim, H. Choi, C. Baik, K. Song, S. O. Kang and J. Ko, *Tetrahedron*, 2007, **63**, 11436–11443; (*c*) I. Jung, J. K. Lee, K. H. Song, K. Song, S. O. Kang and J. Ko, *J. Org. Chem.*, 2007, **72**, 3652–3658.

13 (*a*) S. Ferrere, A. Zaban and B. A. Greg, *J. Phys. Chem. B*, 1997, **101**, 4490–4493; (*b*) S. Ferrere and B. A. Greg, *New J. Chem.*, 2002, **26**, 1155–1160; (*c*) Y. Shibano, T. Umeyama, Y. Matano and H. Imahori, *Org. Lett.*, 2007, **9**, 1971–1974.

14 (*a*) A. Ehret, L. Stuhl and M. T. Spitler, *J. Phys. Chem. B*, 2001, **105**, 9960–9965; (*b*) S. Ushiroda, N. Ruzycki, Y. Lu, M. T. Spitler and B. A. Parkinson, *J. Am. Chem. Soc.*, 2005, **127**, 5158–5168; (*c*) S. Tatay, S. A. Haque, B. O'Regan, J. R. Durrant, W. J. H. Verhees, J. M. Kroon, A. Vidal-Ferran, P. GaviCa and E. Palomares, *J. Mater. Chem.*, 2007, **17**, 3037–3044.

15 (*a*) M. Velusamy, K. R. J. Thomas, J. T. Lin, Y. Hsu and K. Ho, *Org. Lett.*, 2005, **7**, 1899–1902; (*b*) D. P. Hagberg, T. Edvinsson, T. Marinado, G. Boschloo, A. Hagfeldt and L. Sun, *Chem. Commun.*, 2006, 2245–2247; (*c*) M. Liang, W. Xu, F. Cai, P. Chen, B. Peng, J. Chen and Z. Li, *J. Phys. Chem. C*, 2007, **111**, 4465–4472.

16 (*a*) T. Hasobe, H. Imahori, P. V. Kamat, T. K. Ahn, S. K. Kim, D. Kim, A. Fujimoto, T. Hirakawa and S. Fukuzumi, *J. Am. Chem. Soc.*, 2005, **127**, 1216–1228; (*b*) A. Huijser, T. J. Savenije, A. Kotlewski, S. J. Picken and L. D. A. Siebbeles, *Adv. Mater.*, 2006, **18**, 2234–2239; (*c*) G. M. Hasselman, D. F. Watson, J. R. Stromberg, D. F. Bocian, D. Holten, J. S. Lindsey and G. J. Meyer, *J. Phys. Chem. B*, 2006, **110**, 25430–25440; (*d*) H. Imahori, S. Hayashi, H. Hayashi, A. Oguro, S. Eu, T. Umeyama and Y. Matano, *J. Phys. Chem. C*, 2009, **113**,

18406–18413; (*e*) J. K. Park, J. Chen, H. R. Lee, S. W. Park, H. Shinokubo, A. Osuka and D. Kim, *J. Phys. Chem. C*, 2009, **113**, 21956–21963.

17 W. M. Campbell, A. K. Burrell, D. L. Officer and K. W. Jolley, *Coord. Chem. Rev.*, 2004, **248**, 1363–1379.

18 M. Tanaka, S. Hayashi, S. Eu, T. Umeyama, Y. Matano and H. Imahori, *Chem. Commun.*, 2007, 2069–2071.

19 (*a*) T. Ripolles-Sanchis, B.-C. Guo, H.-P. Wu, T.-Y. Pan, H.-W. Lee, S. R. Raga, F. Fabregat-Santiago, J. Bisquert, C.-Y. Yeh and E. W.-G. Diau, *Chem. Commun.*, 2012, **48**, 4368–4370; (*b*) H. Imahori, S. Kang, H. Hayashi, M. Haruta, H. Kurata, S. Isoda, S. E. Canton, Y. Infahsaeng, A. Kathiravan, T. Pascher, P. Chábera, A. P. Yartsev and V. Sundström, *J. Phys. Chem. A*, 2011, **115**, 3679–3690.

20 J. N. Clifford, E. Martínez-Ferrero, A. Viterisi and E. Palomares, *Chem. Soc. Rev.*, 2011, **40**, 1635–1646.

21 (*a*) H.-P. Lu, C.-Y. Tsai, W.-N. Yen, C.-P. Hsieh, C.-W. Lee, C.-Y. Yeh and E. W.-G. Diau, *J. Phys. Chem. C*, 2009, **113**, 20990–20997; (*b*) C.-P. Hsieh, H.-P. Lu, C.-L. Chiu, C.-W. Lee, S.-H. Chuang, C.-L. Mai, W.-N. Yen, S.-J. Hsu, E. W.-G. Diau and C.-Y. Yeh, *J. Mater. Chem.*, 2010, **20**, 1127–1134; (*c*) C.-W. Lee, H.-P. Lu, C.-M. Lan, Y.-L. Huang, Y.-R. Liang, W.-N. Yen, Y.-C. Liu, Y.-S. Lin, E. W.-G. Diau and C.-Y. Yeh, *Chem.–Eur. J.*, 2009, **15**, 1403–1412.

22 T. Bessho, S. M. Zakeeruddin, C.-Y. Yeh, E. W.-G. Diau and M. Grätzel, *Angew. Chem., Int. Ed.*, 2010, **49**, 6646–6649.

23 H.-P. Lu, C.-L. Mai, C.-Y. Tsia, S.-J. Hsu, C.-P. Hsieh, C.-L. Chiu, C.-Y. Yeh and E. W.-G. Diau, *Phys. Chem. Chem. Phys.*, 2009, **11**, 10270–10274.

24 E. M. Barea, V. Gónzalez-Pedro, T. Ripollés-Sanchis, H.-P. Wu, L.-L. Li, C.-Y. Yeh, E. W.-G. Diau and J. Bisquert, *J. Phys. Chem. C*, 2011, **115**, 10898–10902.

25 C.-M. Lan, H.-P. Wu, T.-Y. Pan, C.-W. Chang, W.-S. Chao, C.-T. Chen, C.-L. Wang, C.-Y. Lin and E. W.-G. Diau, *Energy Environ. Sci.*, 2012, **5**, 6460–6464.

26 A. Yella, H.-W. Lee, H. N. Tsao, C. Yi, A. K. Chandiran, M. K. Kazeeruddin, E. W.-G. Diau, C.-Y. Yeh, S. M. Zakeeruddin and M. Grätzel, *Science*, 2011, **334**, 629–634.

27 Y.-C. Chang, C.-L. Wang, T.-Y. Pan, S.-H. Hong, C.-M. Lan, H.-H. Kuo, C.-F. Lo, H.-Y. Hsu, C.-Y. Lin and E. W.-G. Diau, *Chem. Commun.*, 2011, **47**, 8910–8912.